

Electric Field Integral Equations for Electromagnetic Scattering Problems With Electrically Small and Electrically Large Regions

Benjamin D. Braaten, *Student Member, IEEE*, Robert M. Nelson, *Senior Member, IEEE*, and Maqsood A. Mohammed, *Senior Member, IEEE*

Abstract—Numerically stable electric field integral equations (EFIE) are presented for electromagnetic scattering problems that may include both electrically small geometrically complex and electrically large regions. A reduced integrand is achieved by implementing quasi-static assumptions in the electrically small regions, full-wave methods in the electrically large regions, and applying appropriate coupling relations between the regions. Use of the method provides computational efficiency as well as insight into the conditions under which the electromagnetic fields within electrically small regions of the problem can be assumed to be primarily capacitive or inductive in nature. The theoretical development of the method is highlighted in this communication and then applied to examples of electrically small, inductively-loaded, and capacitively-loaded monopole antennas. The accuracy of the results is verified with two independent methods.

Index Terms—Hybrid solution methods, method of moments (MoM), scattering.

I. INTRODUCTION

ELECTROMAGNETIC waves impinging on a body in space may induce surface currents on that body, which produce a scattered field. One method of determining the magnitude and phase of the scattered field is to establish and solve a set of integral equations for the unknown surface currents and charges [1]. Once these induced currents and charges are determined, the scattered field can be evaluated. The application of such concepts has been carried out for years using techniques such as the method of moments (MoM) [2]. Although used for many types of problems, it has been noted that application of full-wave techniques to electrically small, geometrically complex problems can lead to numerical instability [3].

Previous authors [3]–[5] have shown that certain simplifying assumptions are reasonable for problems with both electrically large and electrically small regions that may be geometrically complex and contain multiple types of material. For such problems, it has been shown that employing quasi-static equations

in the electrically small regions, full-wave methods in the remaining regions and appropriately coupling the regions provides solution improvements that include improved numerical efficiency via using a reduced quasi-static Green's function, reduction of the number of unknowns to a single scalar (ρ_s) (rather than up to two vector unknowns if full-wave techniques are used throughout), and reduction of numerical difficulties associated with solving electrically small problems using full-wave techniques [3]–[5]. This technique has been called the *hybrid quasi-static/full-wave method* [4] and was previously limited to problems that exhibited axial symmetry and had electrically small regions in which magnetic induction effects could be ignored.

In this work, the *hybrid quasi-static/full-wave method* developed by Olsen, Hower, and Mannikko has been re-visited. All original equations have been re-derived, Matlab-based computer code has been developed and significant new work has been undertaken. The primary goal of this work is to significantly extend the applicability of the method to general cases that exhibit both inductive and capacitive effects in the electrically small regions.

As such, the method can now be used to model a host of problems that involve both electrically large conducting objects and electrically small, geometrically complex regions. Examples of problems include any type of “large” metal structure (e.g., VLF antenna system, high-voltage power line, aircraft or weapon systems, cabling between electronic systems, etc.) that might also have “small” regions (e.g., insulators, radomes, passive circuits, etc.). In addition to providing a means of solving such problems, the work also provides insight into the conditions under which the electromagnetic fields within an electrically small region of the problem can be assumed to be primarily capacitive or inductive in nature. Understanding this can have a marked influence on the choice of methods used to minimize undesirable effects (i.e., electromagnetic interference) [6], [7]. This insight also paves the way for future work involving lumped-element modeling (i.e., use of the method to derive equivalent circuit parameters). In the process of achieving this primary goal, all of the computational advantages previously cited have been preserved.

II. DERIVATION OF THE EFIE

Consider the geometry of the general electromagnetics problem shown in Fig. 1. The problem consists of four distinct linear, homogeneous, isotropic regions. Regions 1 and 2 are

Manuscript received August 30, 2005; revised August 23, 2007.

B. D. Braaten and R. M. Nelson were with the Department of Electrical and Computer Engineering, North Dakota State University, Fargo, ND 58105 USA and also with Jacobs Technology, Inc., Eglin AFB, FL 32542 USA. They are now with the Department of Electrical and Computer Engineering, North Dakota State University, Fargo, ND 58105 USA (e-mail: r.m.nelson@ieee.org).

M. A. Mohammed is with the TEAS Group, Jacobs Technology, Inc., Eglin AFB, FL 32542 USA.

Digital Object Identifier 10.1109/TAP.2007.912941

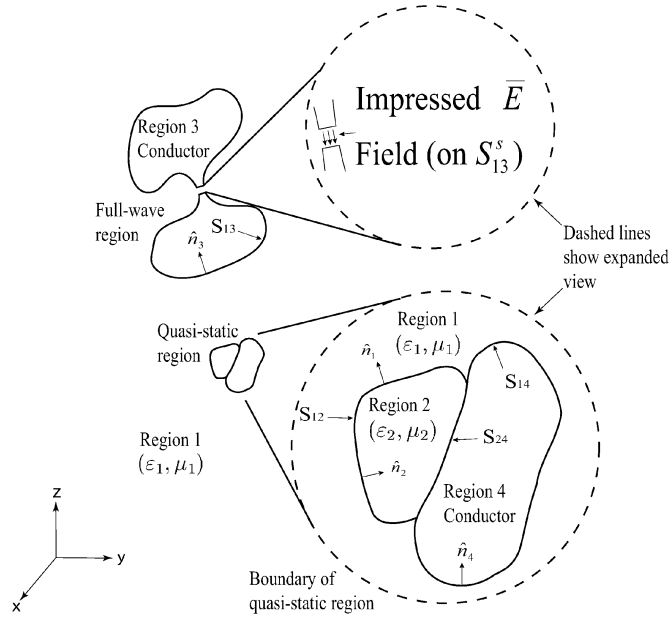


Fig. 1. General electromagnetics problem.

assumed lossless, characterized by the respective values of permittivity and permeability. Regions 3 and 4 are assumed to be perfect conductors. In Fig. 1 it is important to note that the dashed lines show expanded views of selected regions. Note also that region 1 is the unbounded space surrounding the other three regions—which might be entirely in the full-wave region, or partly in the full-wave region and partly in the quasi-static region. Lastly, it should be noted that region 3 can be directly connected to region 1, 2 or 4. In terms of the equations that follow S_{ij} denotes the smooth surface between regions i and j . \vec{r} denotes the vector measured from an arbitrary coordinate system defined on the general electromagnetics problem and \hat{n}_i denotes the unit normal vector in the same coordinate system pointing *into* the i th region. The i th region has permittivity $\varepsilon_i = \varepsilon_{r_i} \varepsilon_0$ and permeability $\mu_i = \mu_{r_i} \mu_0$; and on the subsurface $S_{13}^s \subset S_{13}$ there exists an impressed electric field representing a source in the region. The electric field for \vec{r} in the i th region can be written as [3]

$$\vec{E}_i(\vec{r}) = T \oint_{\partial_i} \vec{Q}_i ds' \quad (1)$$

where

$$\vec{Q}_i = \frac{-1}{4\pi} [j\omega\mu_i(\hat{n}'_i \times \vec{H}_i)\phi_i - (\hat{n}'_i \times \vec{E}_i) \times \nabla' \phi_i - (\hat{n}'_i \cdot \vec{E}_i) \nabla' \phi_i] \quad (2)$$

and

$$\phi_i = \frac{e^{-jk_i R}}{R} \quad (3)$$

and $R = |\vec{r} - \vec{r}'|$, and $k_i = \omega\sqrt{\mu_i\varepsilon_i}$. Equation (1) assumes that there are no volume sources defined in the problem. Also, the fields in (1) and (2) are assumed to vary with $e^{j\omega t}$ and ∂_i indicates that the integral is evaluated over all the smooth surfaces

bounding the i th region of interest (note that the integral is a principle value integral [8], [9]). The primed vectors represent the source points and the unprimed vectors represent the field points. T takes on the values of 1 and 2 in the following manner [3]: $T = 1$ if \vec{r} and \vec{r}' are within region i and $T = 2$ if \vec{r} is on the smooth boundary surface of the region containing \vec{r}' .

In this work, we are interested in solving the general problem defined by (1)–(3) for scenarios that involve both electrically large and electrically small regions (which may be geometrically complex and characterized by finite values of permittivity and permeability). As mentioned earlier, dividing such problems into the electrically large and electrically small regions not only offers computational advantages but also provides the opportunity to investigate whether the electromagnetic fields in electrically small regions are predominantly capacitive or inductive in nature. To facilitate modeling such problems, we will henceforth assume that regions 2 and 4 are electrically small and region 3 is electrically large.

A. Quasi-Static Equations

Note that (1)–(3) indicate that the electric field in the i th region can be expressed in terms of surface integrals evaluated over all surfaces bounding that region. As such, a few approximations can be made if both the field points and source points are in the same quasi-static region. Assume D is the overall maximum dimension of the quasi-static region. If the field point is in region 1 or region 2 of the quasi-static region, and if $k_i D \ll 1$, then $k_i R \leq k_i D \ll 1$. This then gives $e^{-jk_i R} \approx 1$.¹

Thus for $i = 1$ or 2 (3) can be written as

$$\phi_i \approx \frac{1}{R}. \quad (4)$$

This approximation greatly reduces the kernel of the electric field integral equations (EFIE) in the quasi-static regions and provides a considerable gain in computational efficiency and stability over the full-wave version [3]. For this situation, $\nabla\phi_i$ can be written as

$$\nabla\phi_i \approx -\frac{\vec{R}}{R^3} \quad (5)$$

where $\vec{R} = (x - x')\hat{a}_x + (y - y')\hat{a}_y + (z - z')\hat{a}_z$ is the vector from the source point to the field point. This also gives

$$\nabla'\phi_i = -\nabla\phi_i. \quad (6)$$

With these approximations (2) can be written as

$$\vec{Q}_{i,\text{quasi}} = \frac{-1}{4\pi} \left[j\omega\mu_i(\hat{n}'_i \times \vec{H}_i) \frac{1}{R} - (\hat{n}'_i \times \vec{E}_i) \times \frac{\vec{R}}{R^3} - (\hat{n}'_i \cdot \vec{E}_i) \frac{\vec{R}}{R^3} \right]. \quad (7)$$

To evaluate the new EFIE a general expression for the electric field needs to be determined. Consider regions 1 and 2 in Fig. 1.

¹Lossless regions are assumed in this work. The efficacy of using complex material constants to account for loss will be examined in the future by evaluating this approximation when k is complex.

Using (1), if \bar{r} is in the quasi-static region (i.e., $k_1 D \ll 1$) the electric field in region 1 can be written as

$$\bar{E}_1(\bar{r}) = T \int_{S_{13}} \bar{Q}_1 ds' + T \int_{S_{12}} \bar{Q}_{1,\text{quasi}} ds' + T \int_{S_{14}} \bar{Q}_{1,\text{quasi}} ds'. \quad (8)$$

Similarly, the electric field in region 2 can be written as

$$\bar{E}_2(\bar{r}) = T \int_{S_{24}} \bar{Q}_{2,\text{quasi}} ds' + T \int_{S_{24}} \bar{Q}_{2,\text{quasi}} ds'. \quad (9)$$

Since $\bar{E}_i(\bar{r}) = 0$ for \bar{r} not in region i , a general expression for the electric field in the quasi-static region can be written as [10]

$$\bar{E}_i(\bar{r}) = \bar{E}_1(\bar{r}) + \bar{E}_2(\bar{r}). \quad (10)$$

Employing the boundary conditions $\hat{n}'_1 \times [\bar{E}_1 - \bar{E}_2] = 0$, $\hat{n}'_1 \times [\bar{H}_1 - \bar{H}_2] = 0$ and $\varepsilon_1[\hat{n}'_1 \cdot \bar{E}_1] = \varepsilon_2[\hat{n}'_1 \cdot \bar{E}_2]$ on S_{12} and noting that $\hat{n}'_1 = -\hat{n}'_2$ on S_{12} and $\hat{n}'_i \times \bar{E}_i = 0$ on S_{i4} for $i = 1$ and 2 allows one to write (10) as [11]

$$\begin{aligned} \bar{E}_i(\bar{r}) = T & \left[\bar{E}_{\text{inc}} \right. \\ & + \frac{-1}{4\pi} \int_{S_{14}} \left[j\omega\mu_1(\hat{n}'_1 \times \bar{H}_1) \frac{1}{R} - (\hat{n}'_1 \cdot \bar{E}_1) \frac{\bar{R}}{R^3} \right] ds' \\ & + \frac{-1}{4\pi} \int_{S_{24}} \left[j\omega\mu_2(\hat{n}'_2 \times \bar{H}_2) \frac{1}{R} - (\hat{n}'_2 \cdot \bar{E}_2) \frac{\bar{R}}{R^3} \right] ds' \\ & + \frac{-1}{4\pi} \int_{S_{12}} \left[j\omega(\mu_1 - \mu_2)(\hat{n}'_1 \times \bar{H}_1) \frac{1}{R} \right] ds' \\ & \left. + \frac{1}{4\pi} \frac{\varepsilon_{r2} - \varepsilon_{r1}}{\varepsilon_{r2}} \int_{S_{12}} (\hat{n}'_1 \cdot \bar{E}_1) \frac{\bar{R}}{R^3} ds' \right] \quad (11) \end{aligned}$$

where

$$\begin{aligned} \bar{E}_{\text{inc}} = \int_{S_{13}} & \frac{-1}{4\pi} [j\omega\mu_1(\hat{n}'_1 \times \bar{H}_1)\phi_1 \\ & - (\hat{n}'_1 \times \bar{E}_1) \times \nabla' \phi_1 - (\hat{n}'_1 \cdot \bar{E}_1) \nabla' \phi_1] ds'. \quad (12) \end{aligned}$$

Notice that the approximation in (4) is not used in (12). This is because the source points are in the full-wave region and not in the same quasi-static region. Also notice that the expressions

$$j\omega\mu_1(\hat{n}'_1 \times \bar{H}_1) \frac{1}{R}$$

$$j\omega\mu_2(\hat{n}'_2 \times \bar{H}_2) \frac{1}{R}$$

and

$$j\omega(\mu_1 - \mu_2)(\hat{n}'_1 \times \bar{H}_1) \frac{1}{R}$$

represent the magnetic inductive effects. These terms were assumed negligible in earlier work [3], [4].

B. Material Interfaces Within the Quasi-Static Region

Using $T = 2$ in the expression for the electric field in (11), the boundary condition $\hat{n}'_1 \cdot [\varepsilon_1 \bar{E}_1 - \varepsilon_2 \bar{E}_2] = 0$ is enforced at point

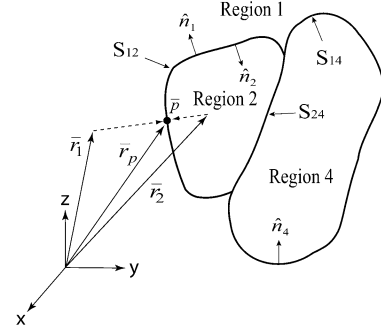


Fig. 2. Boundary limit for the EFIE in the quasi-static region.

\bar{p} on S_{12} shown in Fig. 2. To evaluate this boundary condition at \bar{p} , the limits [10], [11]

$$L_1 = \lim_{\bar{r}_1 \rightarrow \bar{r}_p} \varepsilon_{r1} \hat{n}_1 \cdot \bar{E}_1(\bar{r}_1) \quad (13)$$

and

$$L_2 = \lim_{\bar{r}_2 \rightarrow \bar{r}_p} \varepsilon_{r2} \hat{n}_1 \cdot \bar{E}_2(\bar{r}_2) \quad (14)$$

are evaluated with $\bar{r}_1 \rightarrow \bar{r}_p$ from region 1 along the dotted normal vector and $\bar{r}_2 \rightarrow \bar{r}_p$ from region 2 along the dotted normal vector in Fig. 2.

Subtracting (14) from (13) and solving for $\hat{n}_1 \cdot \bar{E}_{\text{inc}}(\bar{r}_p)$ gives [10]–[13]

$$\begin{aligned} \hat{n}_1 \cdot \bar{E}_{\text{inc}}(\bar{r}_p) = & \hat{n}_1 \\ & \cdot \frac{1}{4\pi} \int_{S_{14}} \left[j\omega\mu_1(\hat{n}'_1 \times \bar{H}_1) \frac{1}{R} - (\hat{n}'_1 \cdot \bar{E}_1) \frac{\bar{R}}{R^3} \right] ds' \\ & + \hat{n}_1 \cdot \frac{1}{4\pi} \int_{S_{24}} \left[j\omega\mu_2(\hat{n}'_2 \times \bar{H}_2) \frac{1}{R} - (\hat{n}'_2 \cdot \bar{E}_2) \frac{\bar{R}}{R^3} \right] ds' \\ & + \left(\frac{\varepsilon_{r1} + \varepsilon_{r2}}{2\varepsilon_{r2}} \right) (\hat{n}_1 \cdot \bar{E}_1(\bar{r}_p)) \\ & + \hat{n}_1 \cdot \left(\frac{\varepsilon_{r1} - \varepsilon_{r2}}{4\pi\varepsilon_{r2}} \right) \int_{S_{12}} (\hat{n}'_1 \cdot \bar{E}_1) \frac{\bar{R}}{R^3} ds' \\ & + \hat{n}_1 \cdot j\omega(\mu_1 - \mu_2) \frac{1}{4\pi} \int_{S_{12}} (\hat{n}'_1 \times \bar{H}_1) \frac{1}{R} ds' \quad (15) \end{aligned}$$

for \bar{r}_p (or \bar{r}) on S_{12} . The tangential components of the magnetic fields in (15) are continuous across S_{12} [13] and are related to the polarization surface current [14] on S_{12} and total surface currents on S_{14} and S_{24} . Thus a direct subtraction of (14) from (13) gives the three integrands in (15) for the tangential magnetic fields. The normal components of the electric fields in (15) are discontinuous across S_{12} and are related to the polarization surface charge on S_{12} and total surface charge on S_{14} and S_{24} . The third term on the right hand side of (15) is due to the discontinuity of the normal components across S_{12} [11].

C. Conductor Interfaces Within the Quasi-Static Region

The next boundary condition to be enforced is $\hat{n}_1 \times \bar{E}_1 = 0$ on S_{14} . Using (5) and (11) the boundary condition for the electric field is

$$\hat{n}_1 \times \bar{E}_1(\bar{r}) = 0 = \hat{n}_1 \times (-j\omega \bar{A}_{\text{tot}} - \nabla \psi_{\text{tot}} + \bar{E}_{\text{inc}}) \quad (16)$$

where

$$\begin{aligned} \bar{E}_{\text{inc}} &= \frac{-j\omega\mu_1}{4\pi} \int_{S_{13}} (\hat{n}'_1 \times \bar{H}_1) \phi_1 ds' \\ &\quad - \nabla \frac{1}{4\pi} \int_{S_{13}} (\hat{n}'_1 \cdot \bar{E}_1) \phi_1 ds' \end{aligned} \quad (17)$$

and

$$\begin{aligned} \bar{A}_{\text{tot}} &= \frac{\mu_1}{4\pi} \int_{S_{14}} (\hat{n}'_1 \times \bar{H}_1) \frac{1}{R} ds' \\ &\quad + \frac{\mu_2}{4\pi} \int_{S_{24}} (\hat{n}'_2 \times \bar{H}_2) \frac{1}{R} ds' \\ &\quad + (\mu_1 - \mu_2) \frac{1}{4\pi} \int_{S_{12}} (\hat{n}'_1 \times \bar{H}_1) \frac{1}{R} ds' \end{aligned} \quad (18)$$

and

$$\begin{aligned} \psi_{\text{tot}} &= \frac{1}{4\pi} \int_{S_{14}} (\hat{n}'_1 \cdot \bar{E}_1) \frac{1}{R} ds' \\ &\quad + \frac{1}{4\pi} \int_{S_{24}} (\hat{n}'_2 \cdot \bar{E}_2) \frac{1}{R} ds' \\ &\quad + \frac{\varepsilon_{r2} - \varepsilon_{r1}}{\varepsilon_{r2}} \frac{1}{4\pi} \int_{S_{12}} (\hat{n}'_1 \cdot \bar{E}_1) \frac{1}{R} ds'. \end{aligned} \quad (19)$$

Equation (18) is the term that represents the inductive effects in the quasi-static region which were assumed negligible for the cases considered by Olsen, Hower, and Mannikko [3], [4]. A similar relation exists for \bar{r} on S_{24} .

D. Full-Wave Equations

Consider the conductor interfaces in the full-wave region. Using the equivalence theorem the expression for the electric field in region 1 can be written as

$$\begin{aligned} \bar{E}_1(\bar{r}) &= \frac{-j\omega\mu_1}{4\pi} \int_{S_{13}} (\hat{n}'_1 \times \bar{H}_1) \phi_1 ds' \\ &\quad + \nabla' \frac{1}{4\pi} \int_{S_{13}} (\hat{n}'_1 \cdot \bar{E}_1) \phi_1 ds' + \bar{E}^Q(\rho, z). \end{aligned} \quad (20)$$

$\bar{E}^Q(\rho, z)$ is the expression for the electric field from sources on S_{12} , S_{14} , and S_{24} in the quasi-static region and can be written as

$$\bar{E}^Q(\rho, z) = -j\omega\bar{A}_i - \nabla\psi_i \quad (21)$$

with

$$\bar{A}_i = \frac{\mu_1}{4\pi} \int_{S_{i4}+S_{12}} \bar{J}_{si} \phi_i ds' \quad (22)$$

and

$$\psi_i = \frac{1}{4\pi\varepsilon_o} \int_{S_{i4}+S_{12}} \rho_{si} \phi_i ds' \quad (23)$$

where $\bar{J}_{si} = \hat{n}'_i \times \bar{H}_i$ and $\rho_{si}/\varepsilon_o = \hat{n}'_i \cdot \bar{E}_i$ are the surface current and total (free and polarization) surface charge densities, respectively on each surface.

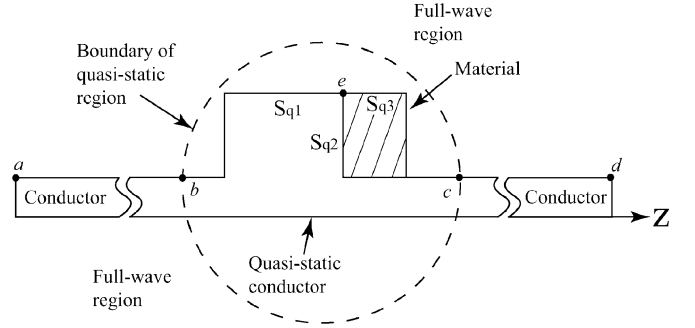


Fig. 3. Enforcement of current continuity equation and conservation of charge.

E. Conductor Interfaces in Full-Wave Region

Using the boundary condition $\hat{n}_1 \times \bar{E}_1(\bar{r}) = 0$ on S_{13} in Fig. 1, the expression for the electric field can be written as

$$\begin{aligned} \hat{n}_1 \times \bar{E}_1(\bar{r}) &= 0 = \hat{n}_1 \\ &\quad \times \left[\frac{-j\omega\mu_1}{4\pi} \int_{S_{13}} (\hat{n}'_1 \times \bar{H}_1) \phi_1 ds' \right. \\ &\quad \left. + \nabla' \frac{1}{4\pi} \int_{S_{13}} (\hat{n}'_1 \cdot \bar{E}_1) \phi_1 ds' + \bar{E}^Q(\rho, z) \right]. \end{aligned} \quad (24)$$

F. Current Continuity and Conservation of Charge

The unknowns in the previous equations include surface charge density in the quasi-static region and surface current density in both regions. These unknowns are related via the conservation of charge and current continuity equation. Consider a completely connected conductor which might lie partly in the full-wave region and partly in the quasi-static region. The conservation of free charge for this conductor is enforced through

$$\varepsilon_{r1} \int_{\sum \partial_m^F} \rho_s(\bar{r}') ds' + \varepsilon_{r2} \int_{\sum \partial_n^Q} \rho_s(\bar{r}') ds' = K \quad (25)$$

where $\sum \partial_n^Q$ is collection of all quasi-static surfaces, $\sum \partial_m^F$ is the collection of all full-wave surfaces, and \bar{r}' is the coordinate along a surface. K is the total free charge on the conductor and is assumed to be zero for our problems. Since current is the only unknown to be determined in the full-wave region, the current continuity equation is used to express the charge in the full-wave region in terms of the current. The continuity equation is

$$\nabla' \cdot \bar{J}_s(\bar{r}') = -j\omega\rho_s(\bar{r}') \quad (26)$$

where \bar{J}_s and ρ_s are the surface current and total surface charge densities on each surface.

Consider the axially symmetric problem in Fig. 3 to help illustrate the use of the current continuity equation and the conservation of charge. It consists of a full-wave region and a quasi-static region that are connected with a conductor. The quasi-static region also has an additional subregion that contains a lossless

material. If we assume that the current in Fig. 3 is axially symmetric and has no azimuthal component, we can write (26) as

$$\frac{dJ_s(l)}{dl} = -j\omega\rho_s(l) \quad (27)$$

where l is a coordinate measured along the surface and $J_s(l)$ is the amplitude of the surface current flowing on the surface at l . Since the only unknown in the full-wave region is current, we will need the integral form of (27) which is expressed in terms of both current and charge

$$J_s(l) - J_s(\tau) = -j\omega \int_{\tau}^l \rho_s(l) dl \quad (28)$$

where $J_s(\tau)$ is the current at either boundary (b or c) of the quasi-static region, and again $J_s(l)$ is the current along the full-wave surface at the coordinate l . (28) is the integration of (27) from either boundary between the two electrical regions to the coordinate l . Thus, multiplying both sides of (25) by $j\omega$ and using (28) we eliminate the need to solve for the charge in the full-wave region.

For example, by making the previous substitution and assuming that the current at the end of the full-wave conductors is zero (i.e., $J_s(l = a) = 0$ and $J_s(l = d) = 0$) and region 1 is free space, we can write

$$J_s(c) - J_s(b) = -j\omega\epsilon_{r_i} \int_{\sum \partial_i^Q} \rho_s(\vec{r}') ds' \quad (29)$$

where $J_s(b)$ and $J_s(c)$ are the transitional currents between the full-wave region and the quasi-static region. (29) enforces the continuity of current between the two electrical regions. It should be noted that the current at the boundaries between the quasi-static regions and full-wave regions is not assumed to be zero. This allows the coupling between different electrical regions to be computed. Special care should be taken while computing these boundary currents. Another place where special care must be exercised is at junctions between perfect conductors and general lossless materials, such as node e in Fig. 3. We note that only free charge exists on S_{q1} , only polarization (or bound) charge exists on S_{q3} , and both exist on S_{q2} . For such instances (25) and (28) are applied to account for free charge, and a modified form is applied a second time to account for polarization (or bound) charge.

If the problem has only full-wave regions then the enforcement of (28) is not needed. The use of (24) without the last term can be used to solve for the desired unknowns. On the other hand if the problem of interest has only quasi-static regions then the enforcement of (25) and (28) is required to solve for the unknowns.

Now (15), (16), (24), (25), and (28) can be solved for the currents and charges in all regions.

III. COMPUTATIONAL EXAMPLES AND CONSIDERATIONS

Having laid the theoretical foundation for the new work we turn to computational aspects. We begin by looking at specific examples which highlight the primary focus of this

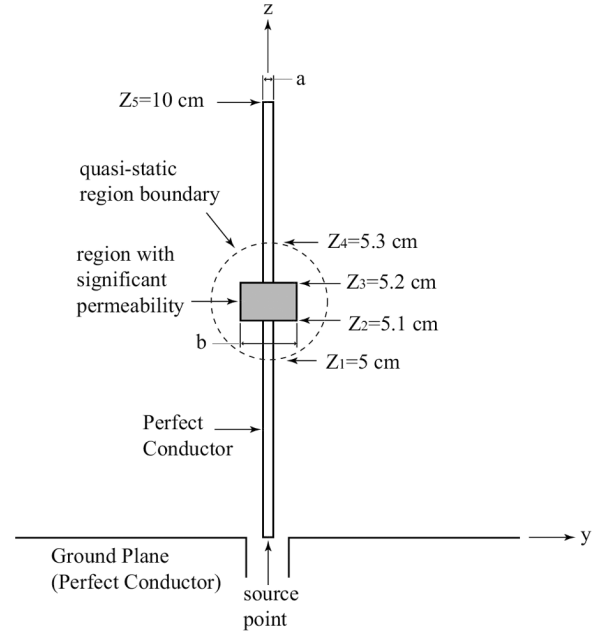


Fig. 4. Inductively loaded monopole.

work—namely to determine the solution of scattering problems that include both electrically large and electrically small regions (which may exhibit both inductive and capacitive effects). We also examine various computational considerations including insights regarding how the number of equations, unknowns, and computational speed compare to full-wave methods, as well as when it may be appropriate to model the effect of the electromagnetic fields within electrically small regions using two-terminal circuit elements. Such insights lay the foundation for future work that may focus directly on using two-terminal circuit elements to model such situations.

A. Computational Examples

The first problem selected to test the new EFIE was the inductively loaded monopole shown in Fig. 4. Part of the quasi-static region in Fig. 4 is a ferrite bead wrapping around a wire. Such beads are often used to introduce inductance [6], [7]. In this problem, the “ferrite bead” region is characterized by $\epsilon_{r_2} = 1.01$ and permeability $\mu_{r_2} = 30$ with $a = 0.15$ mm and $b = 2$ mm. We note that $\epsilon_{r_2} = 1.0$ also provides correct results, but $\epsilon_{r_2} = 1.01$ was used so that the 4th term on the right side of (15) is non-zero.

As implied by the reference to a ferrite bead, this problem was selected because it exhibits significant inductive effects. It is not always clear if the electromagnetic fields in quasi-static regions are primarily inductive or capacitive. Arguments to help determine this are presented in [3] and will be discussed shortly.

The MoM was used to solve the new EFIE. In particular, the point matching technique [19] was chosen. Matlab was used to carry out the MoM implementation. The Matlab code contains subroutines that generate the source and match points, carry out necessary numerical integration, and solve the resulting matrix equation. A Matlab-based graphical user interface (GUI) was written to help manage all the subroutines. The name QUICNEC [11] has been given to this Matlab GUI. QUICNEC

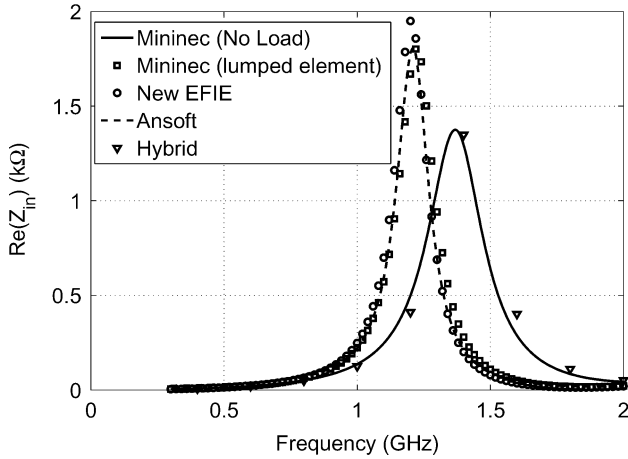


Fig. 5. Input resistance for inductively loaded monopole.

stands for quasi-static inductive capacitive numerical electromagnetics code. The GUI allows the user to easily input an array of axially symmetric problems. (More information on the capabilities and limitations of QUICNEC can be found in [11].) QUICNEC was used to determine the input impedance of the inductively loaded monopole shown in Fig. 4. The number of unknowns was increased until the input impedance converged ($N = 160$ in this case). It should be noted that N is larger than what might typically be expected because both the surface charge density (in the quasi-static region) and surface current density (in both full-wave and quasi-static regions) are being solved for simultaneously.

The results obtained from the new EFIE are compared to the results provided by Mininec Classic [15] and Ansoft [16]. Mininec Classic was used because a lumped element can be calculated to approximate the inductance of the quasi-static region. For the geometry shown in Fig. 4 an equivalent lumped inductor of $L \approx \frac{\mu(z_3 - z_2)}{2\pi} \ln\left(\frac{b}{a}\right)$ was used. (This expression can be derived by determining the energy stored in the magnetic field within the bead, assuming a magnetic field intensity in the bead of $\vec{H} \approx I/(2\pi\rho)\hat{a}_\phi$.) For the problem at hand, a lumped inductance of $L \approx 15.5$ nH was defined in Mininec Classic at a node that corresponded to the center of the quasi-static region in Fig. 4. Results from QUICNEC were also compared to those obtained using Ansoft. Ansoft was chosen for two reasons. First, it provides results using the Finite Element Method [17] which is based on completely different principles than presented here. Secondly, work done by Kennedy, Long, and Williams [18] suggest that solutions to problems similar to this one can be calculated using Ansoft. It should be noted here that the surfaces defined in Ansoft were not smooth. Every surface was defined to be a tetrahedron with 14 sides.

Results for the input impedance of the monopole antenna were obtained using all three methods (QUICNEC, Mininec and Ansoft) for the frequency range of 0.3–2.0 GHz. This frequency range was selected to ensure that the quasi-static assumptions were still valid. The calculated input resistance and reactance are shown in Figs. 5 and 6, respectively. Excellent correlation is noted between the results obtained from the new EFIE (i.e., QUICNEC), Mininec Classic, and Ansoft.

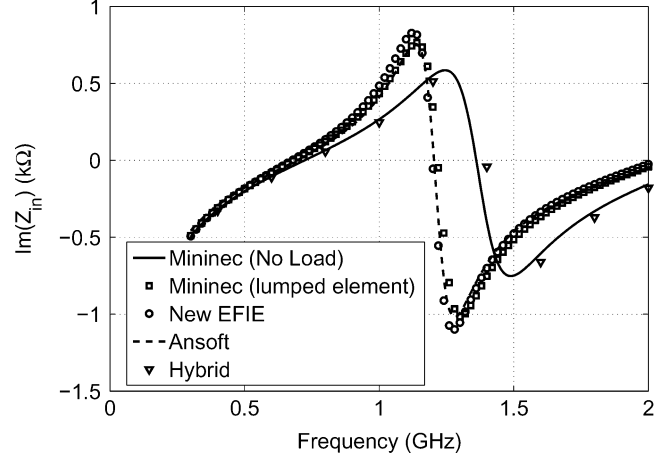


Fig. 6. Input reactance for inductively loaded monopole.

The input impedance of a monopole without a load is also presented in Figs. 5 and 6. Results obtained from the original hybrid method [3]–[5] and those of an unloaded monopole are included to show the significance of the inductive effects. These results suggest that using a two-terminal inductive element to represent the effect of the electromagnetic fields in this region is justified. As such, the capacitive effects in this region can be neglected.

The results shown in Figs. 5 and 6 clearly illustrate the efficacy of the work presented here for problems involving inductive effects. Several other types of problems have been also been examined. The capacitively loaded monopole shown in [3] was simulated using the EFIE described here and in [11]. The results compare very well with measurement results and results obtained from the original hybrid quasi-static/full-wave [3].

Initial results have also been obtained for lossy materials by using complex values of μ and ϵ to account for loss. Although the outcome of these simulations look promising [21], further work needs to be undertaken to provide a rigorous proof of the applicability of using the new EFIE for such cases.

B. Computational Considerations

The primary focus of this work was to extend the applicability of the original hybrid quasi-static/full-wave method to include both inductive and capacitive effects in electrically small regions. This method provides the user with the opportunity of not only solving complex problems, but also being able to investigate if the electromagnetic fields in the quasi-static region are predominantly capacitive or inductive in nature. To examine that question, we note that the relative magnitudes of the first and third terms in (7) can be shown to be $|k_i^2 R^2 \vec{J}_s|$ and $|\nabla \cdot \vec{J}_s \vec{R}|$ respectively. If $|k_i^2 R^2 \vec{J}_s| \ll |\nabla \cdot \vec{J}_s \vec{R}|$ then capacitive effects are dominant in the quasi-static regions [3]. If $|k_i^2 R^2 \vec{J}_s| \gg |\nabla \cdot \vec{J}_s \vec{R}|$ inductive effects are dominant. If $|k_i^2 R^2 \vec{J}_s| \approx |\nabla \cdot \vec{J}_s \vec{R}|$ then both terms need to be considered. If capacitive effects are dominant, $|k_i^2 R^2 \vec{J}_s| \ll |\nabla \cdot \vec{J}_s \vec{R}|$ implies that $|k_i^2 R \vec{J}_s| \ll |\nabla \cdot \vec{J}_s|$. As Olsen points out [3], [4] since $k_i R \ll 1$ within the electrically small region, this inequality will hold whenever $|\nabla \cdot \vec{J}_s|$ is “large”, which implies that \vec{J}_s has significant spacial variation within the region. This will be

true when the current changes rapidly. An example given in [3], [4] is that of a parallel plate capacitor where “the current varies rapidly near the capacitor plates to sustain a build up of charge” [3], [4].

To gain further insight into the capacitive problem, note that (26) implies $|\nabla \cdot \bar{J}_s| = \omega|\rho_s|$. Therefore, capacitive effects are dominant when $\omega|\rho_s| \gg |k_i^2 R \bar{J}_s|$. Since $k_i R \ll 1$ in the electrically small region, if “ \ll ” means a factor of less than or equal to 0.1 (a typical assumption), $|k_i R|_{\max} = 0.1$. Noting that $k_i = \omega\sqrt{\mu_i \varepsilon_i}$, $\omega|\rho_s| \gg |k_i^2 R \bar{J}_s|$ becomes $|\rho_s| > 0.1\sqrt{\mu_i \varepsilon_i} |\bar{J}_s|$. Therefore, capacitive effects are dominant when

$$\frac{|\rho_s|}{|\bar{J}_s|} > 0.1\sqrt{\mu_i \varepsilon_i}. \quad (30)$$

Although (30) provides a description of the relative magnitudes of the surface charge and current for capacitively dominant problems, it does not yield a useful prediction mechanism since these magnitudes are not known a priori. A similar result will occur for problems where inductive effects are dominant. Although it may not be possible to determine if capacitive or inductive effects are dominant a priori, the results presented here can be used to provide meaningful insight for particular problems. One way to check this is to run QUICNEC and then run a modified form of QUICNEC which neglects the inductive effects in (15) and \bar{A}_{tot} in (16) and then compare the results. If negligible changes in the results occur, the effects were predominantly capacitive for that problem. If significant changes occur in the results one can conclude that significant inductive effects occurred. For example, capacitive effects were verified in the case of the capacitively loaded monopole by observing no change in the input impedance when the two versions of QUICNEC were run. For the example of the inductively loaded monopole, very significant changes were observed in the results obtained from the two versions of QUICNEC. This indicates that significant inductive effects are present. Although one cannot definitely say that capacitive effects are negligible, the significant change in results indicates this may be the case. For the particular results shown in Fig. 5 dominant inductive effects are verified by the excellent agreement between the QUICNEC results (i.e., the new EFIE) and those obtained with the other methods. Further work is in progress which will allow the user to determine definitively whether inductive or capacitive effects are dominant for a given problem.

Although the main focus of this work was not to reduce the number of unknowns or decrease computation time, improvement in such aspects were welcome benefits. To examine such issues, consider the equations that need to be solved if one uses traditional full-wave techniques to enforce the boundary conditions on a dielectric-dielectric interface. It can be shown [1] that the resulting equations are

$$\begin{aligned} \hat{n}_1 \times \bar{E}_{\text{inc}} = & \frac{1}{4\pi} \hat{n}_1 \times \int_{S_{12}} j\omega\mu \bar{J}_s (\phi_1 + \phi_2) ds' \\ & + \frac{1}{4\pi} \hat{n}_1 \times \int_{S_{12}} \bar{K}_s \times \nabla' (\phi_1 + \phi_2) ds' \\ & + \frac{1}{4\pi} \hat{n}_1 \times \int_{S_{12}} \frac{1}{j\omega\varepsilon} \nabla' \cdot \bar{J}_s \nabla' (\phi_1 + \frac{\varepsilon_1}{\varepsilon_2} \phi_2) ds' \end{aligned} \quad (31)$$

and

$$\begin{aligned} \hat{n}_1 \times \bar{H}_{\text{inc}} = & \frac{1}{4\pi} \hat{n}_1 \times \int_{S_{12}} j\omega\varepsilon \bar{K}_s (\phi_1 + \frac{\varepsilon_1}{\varepsilon_2} \phi_2) ds' \\ & - \frac{1}{4\pi} \hat{n}_1 \times \int_{S_{12}} \bar{J}_s \times \nabla' (\phi_1 + \phi_2) ds' \\ & + \frac{1}{4\pi} \hat{n}_1 \times \int_{S_{12}} \frac{1}{j\omega\mu} \nabla' \cdot \bar{K}_s \nabla' (\phi_1 + \phi_2) ds'. \end{aligned} \quad (32)$$

where $\bar{J}_s = \hat{n} \times \bar{H}$, $\bar{K}_s = -\hat{n} \times \bar{E}$ and ϕ_i is given in (3). If ρ_s is obtained using the current continuity equation one needs to solve 5 equations with 5 unknowns (i.e., two components of both \bar{J}_s and \bar{K}_s , along with ρ_s). In contrast, (15) is the equation enforced on the dielectric-dielectric interfaces in the quasi-static regions, which results in one equation and three unknowns (i.e., two components of $\hat{n}'_i \times \bar{H}_i$, along with ρ_s). For a general quasi-static problem, the other two equations are obtained by applying (29) to each component of \bar{J}_s . Thus application of this method to general dielectric-dielectric interfaces reduces the problem from solving 5 scalar equations to 3 scalar equations for each surface. Note that the number of unknowns for both methods are reduced if azimuthal currents are neglected (such as in thin-wire problems).

In addition to reducing the number of equations and unknowns, it is important to note that the integrands within the new EFIE are less complex than those in the full-wave method described by (31) and (32). Each of the full-wave integrands involve terms with either ϕ_i or $\nabla' \phi_i$ but in (15) the corresponding quasi-static equation involves the $1/R$ and \bar{R}/R^3 terms, which result in decreased computation time. Therefore, the method presented here results in fewer unknowns for the quasi-static regions, and reduced computational burden for a given number of unknowns. We point out that the equations used to enforce the boundary condition on the conductor-dielectric interface will yield the same number of unknowns for both the full-wave and quasi-static versions of the EFIE. For instance, (16) will yield 3 unknowns (surface charge and two components of surface current) and two equations. The third equation is (26). Although the number of unknowns for the dielectric-conductor interface is the same for both EFIE, the quasi-static integrands will have less computational burden than the corresponding full-wave integrands. To illustrate that fact, we compare computation times when a full-wave code and QUICNEC are both used to evaluate the problem shown in Fig. 7. It consists of a perfectly conducting quasi-static cylinder with $a = .0005\lambda$ and $L = .01\lambda$. The problem was evaluated using Harrington’s full-wave EFIE ([2, Ch. 4]) and our quasi-static EFIE with the current continuity equation. We used the point matching technique with pulse basis functions and solved for the current and charge. The surface charge calculated using the two methods correspond very well with the exception of the source location (which is a common characteristic of the delta source [22]). Now we want to compare the cpu time between the two methods. Table I shows the average cpu time for each N. In both routines we solve for both the current and charge. An average of 56.66 percent less cpu time was realized with the quasi-static EFIE over the full-wave EFIE.

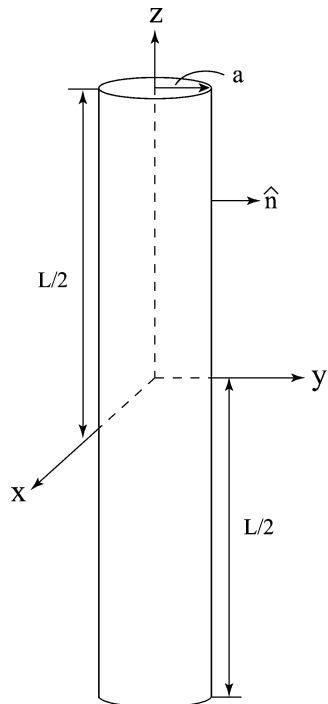


Fig. 7. Quasi-static region.

TABLE I
CPU COMPUTATION TIME

N	Average Quasi-static EFIE CPU Time (ms)	Average Full-wave EFIE CPU Time (ms)	Percent Less CPU Time
8	75.9	182.9	58.6
12	156.3	375.0	58.3
16	216.4	536.5	59.6
20	323.7	656.3	50.6
24	399.7	916.7	56.3

IV. CONCLUSION

An integral equation technique has been successfully developed to compute the fields from scattering problems that may have both quasi-static and full-wave regions. The quasi-static regions are considered electrically small and can consist of geometries and material characteristics with permittivities and permeabilities of unity or greater. A MoM implementation has been carried out in Matlab. Results of the input impedance of an inductively loaded monopole are presented and compared with those obtained using Mininec Classic and Ansoft. Excellent correlation is obtained—verifying that the new integral equations provide accurate, detailed results for quasi-static regions with significant inductive and capacitive effects. Use of the method also provides insight into the conditions under which the electromagnetic fields within electrically small regions can be assumed to be primarily capacitive or inductive. Computational considerations are addressed, which includes a comparison of CPU times required for the new EFIE and a traditional full-wave EFIE to determine the surface charge and current for an electrically small wire. Computational efficiency is noted.

ACKNOWLEDGMENT

The authors would like to thank Dr. R. G. Olsen (Washington State University) for providing a copy of the Fortran code based on the work in [3] and [4]. They would also like to thank the Center for Nanoscale Science and Engineering (CNSE), North Dakota State University, for providing access to Ansoft, which was used to verify results given in this work.

REFERENCES

- [1] R. A. Mittra, Ed., *Computer Techniques for Electromagnetics*. Washington, DC: Hemisphere Publishing, 1987, pp. 159–182.
- [2] R. F. Harrington, *Field Computation by Moment Methods*. Malabar, FL: Krieger Publishing, 1982.
- [3] R. G. Olsen, G. L. Hower, and P. D. Mannikko, “A hybrid method for combining quasi-static and full-wave techniques for electromagnetic scattering problems,” *IEEE Trans. Antennas Propag.*, vol. 36, no. 8, pp. 1180–1184, Aug. 1988.
- [4] R. G. Olsen and P. D. Mannikko, “Validation of the hybrid quasi-static/full-wave method for capacitively loaded thin-wire antennas,” *IEEE Trans. Antennas Propag.*, vol. 38, no. 4, pp. 516–522, Apr. 1990.
- [5] P. D. Mannikko, “Implementation of a full-wave/quasi-static hybrid method for analysis of axially symmetric thin-wire antennas with capacitive loads,” M. S. Thesis, Washington State Univ., Pullman, WA, 1988.
- [6] C. R. Paul, *Introduction to Electromagnetic Compatibility*. New York: Wiley Press, 1990.
- [7] H. W. Ott, *Noise Reduction Techniques in Electronic Circuits*, 2nd ed. New York: Wiley Press, 1988.
- [8] I. S. Gradshteyn and I. M. Ryzhik, *Table of Integrals, Series, and Products*, 6th ed. Boston, MA: Academic Press, 2000, p. 248.
- [9] W. Kaplan, *Advanced Calculus*. Norwood, MA: Addison-Wesley, 1959, p. 578.
- [10] J. Daffe and R. G. Olsen, “An integral equation technique for solving rotationally symmetric electrostatic problems in conducting and dielectric material,” *IEEE Trans. Power Apparatus Syst.*, vol. PAS-98, no. 5, pp. 1609–1616, Sep./Oct. 1979.
- [11] B. D. Braaten, “An integral equation technique for solving electromagnetic problems with electrically small and electrically large regions,” M.S. thesis, North Dakota State Univ., Fargo, N.D., 2005.
- [12] O. D. Kellogg, *Foundations in Potential Theory*. New York: Frederick Ungar, 1929, pp. 160–166.
- [13] J. A. Stratton, *Electromagnetic Theory*. New York: McGraw-Hill, 1941, pp. 464–468.
- [14] H. A. Haus and J. R. Melcher, *Electromagnetic Fields and Energy*. Englewood Cliffs, NJ: Prentice-Hall, 1989, pp. 211–214.
- [15] J. W. Rockway and J. C. Logan, The New MININEC (Version 3): A Mini-Numerical Electromagnetics Code. Springfield, VA, Sep. 1986, U.S. Department of Commerce National Technical Information Service.
- [16] High Frequency Structure Simulator-HFSS v9.2 2003, Ansoft Corporation.
- [17] J. L. Volakis, A. Chatterjee, and L. C. Kempel, *Finite Element Method for Electromagnetics*. New York: IEEE Press, 1998.
- [18] T. F. Kennedy, S. A. Long, and J. T. Williams, “Modification and control of currents on monopole antennas using magnetic bead loading,” *IEEE Antennas Wireless Propag. Lett.*, vol. 2, pp. 208–211, 2003.
- [19] W. L. Stutzman and G. A. Thiele, *Antenna Theory and Design*, 2nd ed. New York: Wiley, 1998, pp. 427–488.
- [20] W. Palm III, *Introduction to MATLAB 6 for Engineers*, 1st ed. New York: McGraw-Hill, 2001.
- [21] B. D. Braaten, Y. Feng, and R. M. Nelson, “High-frequency RFID tags: An analytical and numerical approach for determining the induced currents and scattered fields,” in *Proc. IEEE Int. Symp. Electromagnetic Compatibility*, Portland, OR, Aug. 2006, pp. 58–62.
- [22] G. P. Junker, A. A. Kishk, and A. W. Glisson, “A novel delta gap source model for center fed cylindrical dipoles,” *IEEE Trans. Antennas Propag.*, vol. 43, no. 5, pp. 537–540, May 1995.



Benjamin D. Braaten (S'02) received the B.S. and M.S. degrees in electrical engineering from North Dakota State University, Fargo, in 2002 and 2005, respectively, where he is currently working toward the and M.S. and Ph.D. degrees.

He is a Graduate Research Assistant in the Electrical and Computer Engineering Department at North Dakota State University. While developing this paper, he was employed part-time by Jacobs Technology, Inc., Eglin AFB, FL. His research interests include antennas, methods in computational modeling, issues in electromagnetic compatibility

electromagnetics, source and harmonic analysis.



Robert M. Nelson (M'84–SM'94) received the B.A. degree in mathematics from Northland College, Ashland, WI, in 1977, the M.S.E.E. degree from Washington State University, Pullman, in 1981, and the Ph.D. degree from North Dakota State University (NDSU), Fargo, in 1987.

He is currently a Professor of electrical and computer engineering at NDSU, where he has been a faculty member since 1989. While developing this paper, he was employed part-time by Jacobs Technology, Inc., Eglin AFB, FL. Previously, he

has been a member of technical staff at Bell Telephone Laboratories, has served as a faculty member in the Electrical Engineering Department at the University of Idaho, and has consulted with the Center for Nanoscale Science and Engineering, Fargo, ND; Sverdrup Technology, Eglin Air Force Base; Boston Scientific, Maple Grove, MN; Otter Tail Power Company, Fergus Falls, MN; and the Naval Undersea Warfare Center, New London, CT. He has been working (teaching and research) in the area of applied electromagnetics, including antennas, transmission lines, microwave engineering and electromagnetic interference/compatibility (EMI/EMC) since 1981. He has recently been working on RFID problems—with emphasis on investigating RFID systems using antenna theory and design.

Dr. Nelson is very active in the IEEE EMC Society, currently serving as Chair of the IEEE EMC Education and Student Activities Committee. He has also been active in the IEEE at the regional level, serving in the capacities of Secretary, Vice-Chair and Chair of the IEEE Red River Valley Section.



Maqsood A. Mohammed (M'91–SM'01) received the B.E. degree in electronics and communications engineering from Osmania University, Hyderabad, India, in 1974, and the M.S.E.E. degree and the Ph.D. degree in electrical engineering from Oklahoma University, Norman, in 1976 and 1991, respectively.

He is currently a Technical Fellow in electromagnetic (EM) effects and directed energy at Jacobs Technology, Inc., Eglin AFB, FL, where he has been a member of the technical staff since 1987. Prior to joining Jacobs, he worked in other industries such

as process control, medical instrumentation, and computer peripherals. He has also taught undergraduate courses in electrical engineering as an Adjunct Faculty Member and advised graduate research work at the university level. His expertise is in design, development and testing of electrotechnology systems to achieve electromagnetic compatibility without sacrificing performance. His experience includes various commercial, DoD, and NASA systems. His expertise also includes independent verification and validation (IV&V) of EM and high power microwave (HPM) effects modeling and simulation (M&S) tools. He is a current member of the DETEC HPM IPT for the development of sensors, systems, and tools for HPM test and evaluation and safety. He has been working in the areas of applied electromagnetics including electromagnetic compatibility since 1987 and has developed numerous one-of-a-kind, innovative and unconventional solutions to complicated electromagnetic problems. He has developed solutions to make spread spectrum systems achieve EMC, developed efficient use of congested spectrum at a test range, developed field measurement techniques for extremely narrow and high energy EM pulse trains, developed cost effective ways to test for lightning effects, and developed an innovative V&V methodology for EM modeling and simulation codes. His current research area includes reverberation chambers characterization for HPM signal propagation.

Dr. Mohammed has been very active in the IEEE EMC Society since 1991. He has also been active in the IEEE at the regional level, serving as the Education Outreach officer and also as the Northwest Florida Section Chair. In 1992 he conceived and led the EMC fundamentals tutorial workshop and nurtured it to become the most-attended workshop at the IEEE EMC-S Annual Symposium. During his tenure as Chair of the EMC-S Education and Student Activities Committee (1998–2006), he introduced several new programs and strengthened existing ones such as EMC Fundamentals Tutorial, Student Paper Contest, Student Design Contest, Symposium Experiment Hardware and Software (M&S) Demonstrations, University Grant program, and Tutorial Videos. His long, dedicated and exceptional service to the EMC-S community was recognized by the EMC-S Board and he was awarded the prestigious first ever “Sustained Service to the EMC Society Award” in 2007.